Hydrolytic antibodies: variations on a theme

Gavin MacBeath and Donald Hilvert

Comparison of four independently-derived hydrolytic antibodies reveals striking similarities in their active sites. A common structural motif appears to be induced when the immune system is challenged with antigens containing aryl phosphonate and phosphonamidate groups, and key variations on this 'theme' must account for the observed differences in catalytic efficacy and mechanism. The limited structural repertoire accessed through standard immunization procedures suggests that new approaches may be needed to produce antibody catalysts with enzyme-like efficiencies.

Address: Departments of Chemistry and Molecular Biology, The Scripps Research Institute, La Jolla, CA 92037 USA.

Chemistry & Biology June 1996, **3**:433–445

Introduction

Many biological processes depend on the selective hydrolysis of esters and amides. In nature, efficient and often highly specific enzymes promote these reactions, affording exacting control over such events as blood clotting, fertilization, and complement activation [1–3]. As a result, much effort has been directed towards investigating the basic principles underlying enzyme-catalyzed ester and amide hydrolysis. Many attempts have been made to mimic these systems to test and increase our understanding. One promising approach has tapped the enormous diversity of the mammalian immune system to obtain antibody molecules with tailored hydrolytic properties. Here we review some recent insights into the catalytic mechanism of a number of these antibodies and discuss their implications for generating catalysts with enzyme-like efficiency.

Hydrolytic antibodies

In 1969, Jencks [4] predicted that antibodies elicited against stable analogs of reaction transition states would catalyze the corresponding reactions. Since then, almost 100 antibodies with catalytic properties have been reported [5,6]. Of these, well over half accelerate the hydrolysis of activated ester substrates. Ester and amide hydrolysis is known to involve transient formation of a high energy intermediate which subsequently decomposes to the corresponding acid and alcohol or amine. The high energy intermediate and its flanking transition states can be mimicked effectively using phosphonates or phosphonamidates (Fig. 1). Such analogs resemble the reaction transition states in a number of ways, including tetrahedral geometry, negative charge, and increased bond lengths. Consequently, these molecules have been used widely both as effective

Figure 1

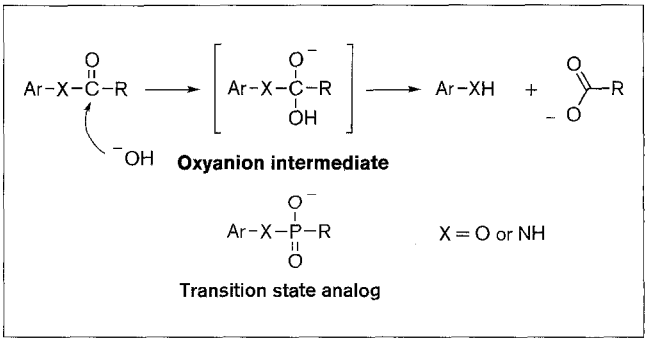

Generalized hydrolysis of an aryl ester or anilide. The corresponding phosphonate (X = O) or phosphonamidate (X = NH) transition state analog mimics the geometric and charge properties of the high energy oxyanion intermediate and its flanking transition states.

inhibitors of hydrolytic enzymes [7–10] and as haptens (immunizing agents) to generate hydrolytic antibodies [5].

Recently, structural information has become available for four different hydrolytic antibodies, affording further insight into the basis of antibody catalysis. The haptens used in these studies and the corresponding reactions are shown in Figure 2. In each case, the same general strategy was employed, namely immunization of a mouse with an arylphosphonate or arylphosphonamidate hapten, followed by monoclonal antibody production using standard hybridoma techniques [11]. The antibodies produced by the hybridoma cell lines were then screened for hapten recognition and for catalytic activity. The four studies were performed independently in different laboratories, using different mice, and different haptens, and the resulting antibodies catalyze their target reactions with significantly different efficiency. Yet when the structures are compared, striking similarities become apparent. The independent experiments did not yield four distinct solutions to the problem of phosphonate (phosphonamidate) binding and ester (amide) hydrolysis, as we might have expected given the enormous diversity of the immune response. Instead, a central 'theme' has emerged upon which are built unique variations that must account for the observed differences in catalytic efficiency and mechanism.

CNJ206: the basic theme

Antibody CNJ206 was generated with phosphonate **1a** and selected for its high affinity binding to the short transition-state analog **1b** [12]. The selection strategy was designed to narrow the pool of antibodies to those that specifically recognized elements of the hapten that program for catalysis. The resulting collection of clones yielded several antibodies that hydrolyze the corresponding activated ester substrate **2b** with rate enhancements

Figure 2

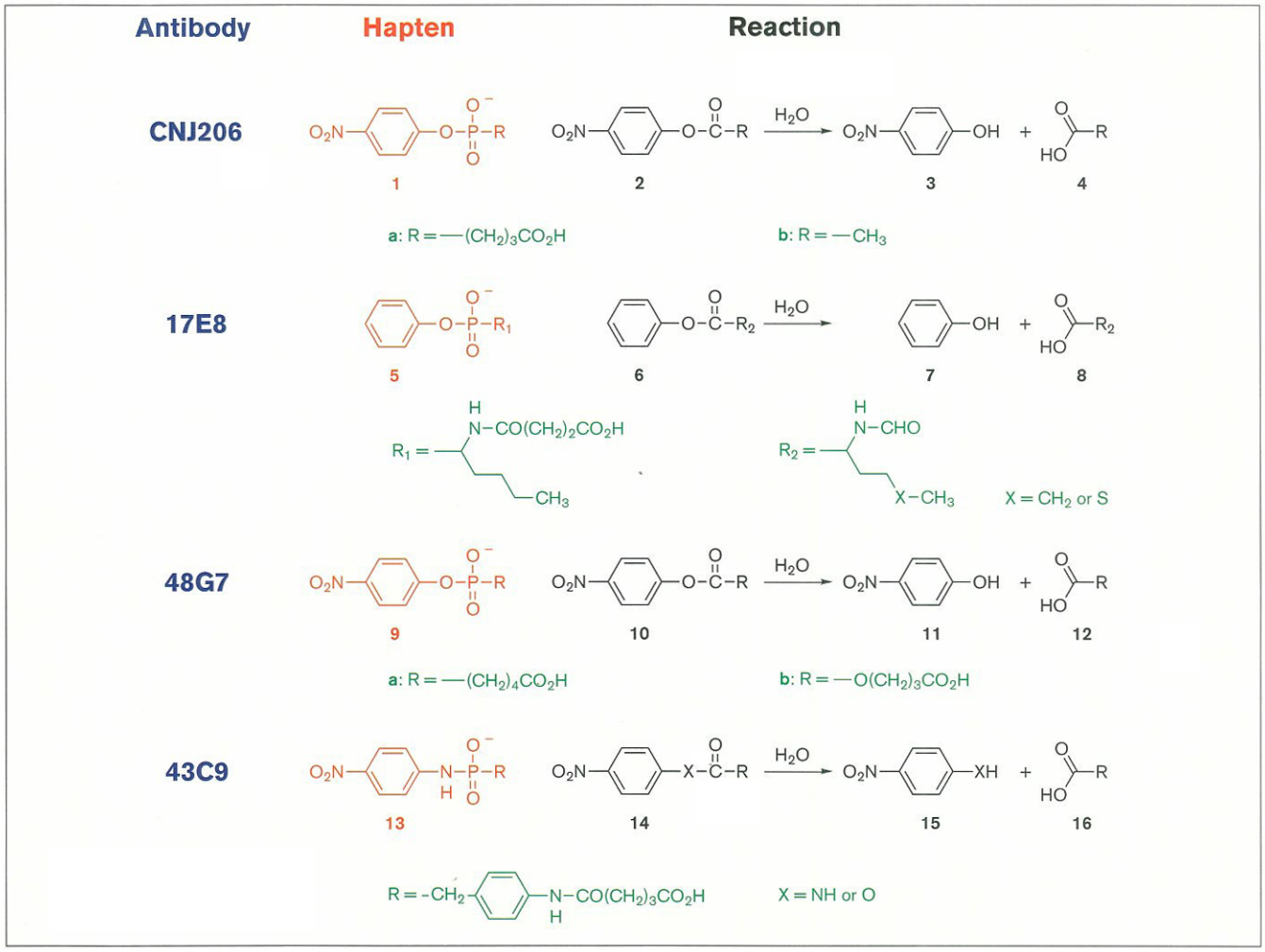

Phosphonate/phosphonamidate haptens used to generate four different hydrolytic antibodies: CNJ206 [12], 17E8 [18], 48G7 [26], and 43C9 [28]. The corresponding reactions catalyzed by the antibodies are shown in black.

(k_{cat}/k_{uncat}) of 10^3–10^4. One of these antibodies, CNJ206, accelerates the hydrolysis of **2b** by a factor of 1600, achieves multiple turnovers, and exhibits substrate specificity consonant with the structure of the inducing hapten.

Recently, the structure of CNJ206 complexed with the short transition-state analog **1b** was solved to 3.2 Å resolution [13]. In addition, the structure of the uncomplexed antibody was solved to 3.0 Å resolution [14], enabling the assessment of ligand-induced conformational changes. Like all antibodies, CNJ206 forms its ligand-binding site chiefly from loops at the end of the variable domains of the heavy (H) and light (L) chains. These loops are known as complementarity-determining regions (CDRs). In the absence of ligand, the binding site of CNJ206 forms a long, shallow groove instead of the deep pocket that is characteristic of antibodies that bind small molecules. The shallowness of the groove results primarily from the orientation of TyrH97 (Tyr97 of the heavy chain, Kabat numbering system [15]), which sits in the active site in such a way as to prevent the formation of a deep cavity.

Upon ligand binding, however, large conformational changes take place in the antibody (Fig. 3) [13]. The variable domains of the heavy and light chains realign, undergoing a 7° rotation with respect to each other and a 0.9 Å translation parallel to the axis of rotation. In addition to this global rearrangement, a significant conformational change is observed in the CDR3 loop of the heavy chain (CDRH3; GlyH95 to TyrH102) (Fig. 3). Notably, the phenyl ring of TyrH97, which occludes the binding pocket in the unliganded antibody, rotates 90° to enlarge the cavity and allow the phosphonate ligand to become engulfed in the active site, where 95 % of its surface is sequestered from solvent.

In the complex, the ligand is oriented with its *p*-nitrophenyl group located at the bottom of a deep, apolar pocket where hydrophobic and van der Waals interactions predominate. Its phosphonate group is located at the mouth of the cavity and forms specific hydrogen bonds with the antibody (Fig. 4a; see also Fig. 6a). The side chain of HisH35 donates one hydrogen bond to the pro-R phosphonate oxygen, while two more hydrogen bonds form between the pro-S oxygen and the backbone NH groups of AspH96 and TyrH97. These observations suggest that CNJ206 functions according to the mechanism programmed by its hapten. It appears to be a relatively simple catalyst that facilitates direct hydroxide attack on the scissile carbonyl of *p*-nitrophenyl esters by stabilizing the oxyanion intermediate and flanking transition states through specific hydrogen bonding interactions. The observed rate acceleration of 1600 corresponds roughly to the contribution of a single oxyanion binding residue in the serine protease subtilisin [16,17].

17E8: a variation on the theme with increased activity

Like CNJ206, antibody 17E8 was generated against an arylphosphonate hapten [18]. In this case, however, the hapten (phosphonate **5**) did not contain a nitro group in the aromatic moiety and differed significantly in the aliphatic side chain (Fig. 2). Antibody 17E8 catalyzes the enantioselective hydrolysis of unactivated phenyl esters of *N*-formyl-L-norleucine (**6**, X = CH_2) and *N*-formyl-L-methionine (**6**, X = S) with rate enhancements of around 10^4 over background (Table 1). It is thus a significantly more active catalyst than CNJ206. The pH–rate profile for

Figure 3

Stereo pair showing the conformational changes that occur in antibody CNJ206 upon binding its hapten. The complexed antibody is shown in white, with its CDRH3 loop in blue and hapten **1b** in orange. The uncomplexed antibody is colored pale green, with its CDRH3 loop bright green. The crystal structures were superimposed using the backbone atoms of residues 1 to 107 of the light chain and residues 1 to 90 of the heavy chain (root-mean-square deviation of 1.06 Å for 1608 atoms).

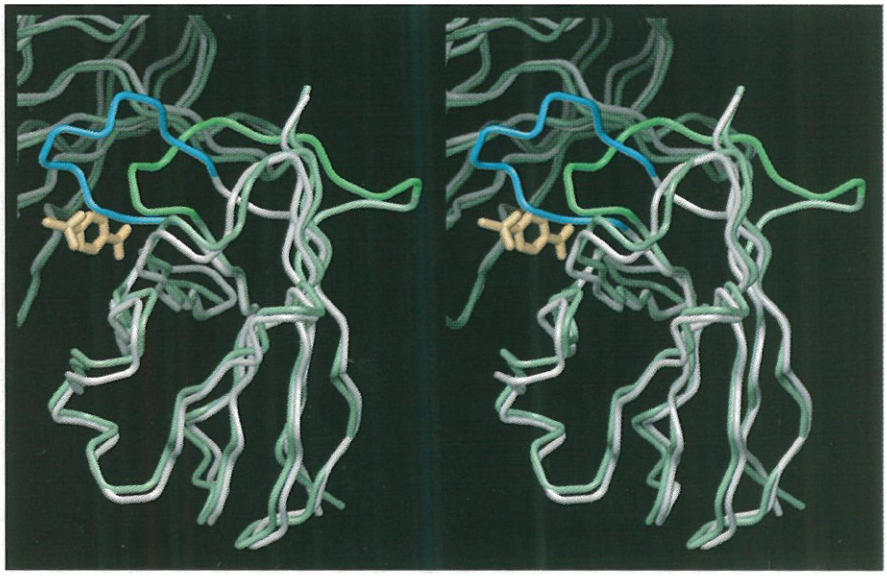

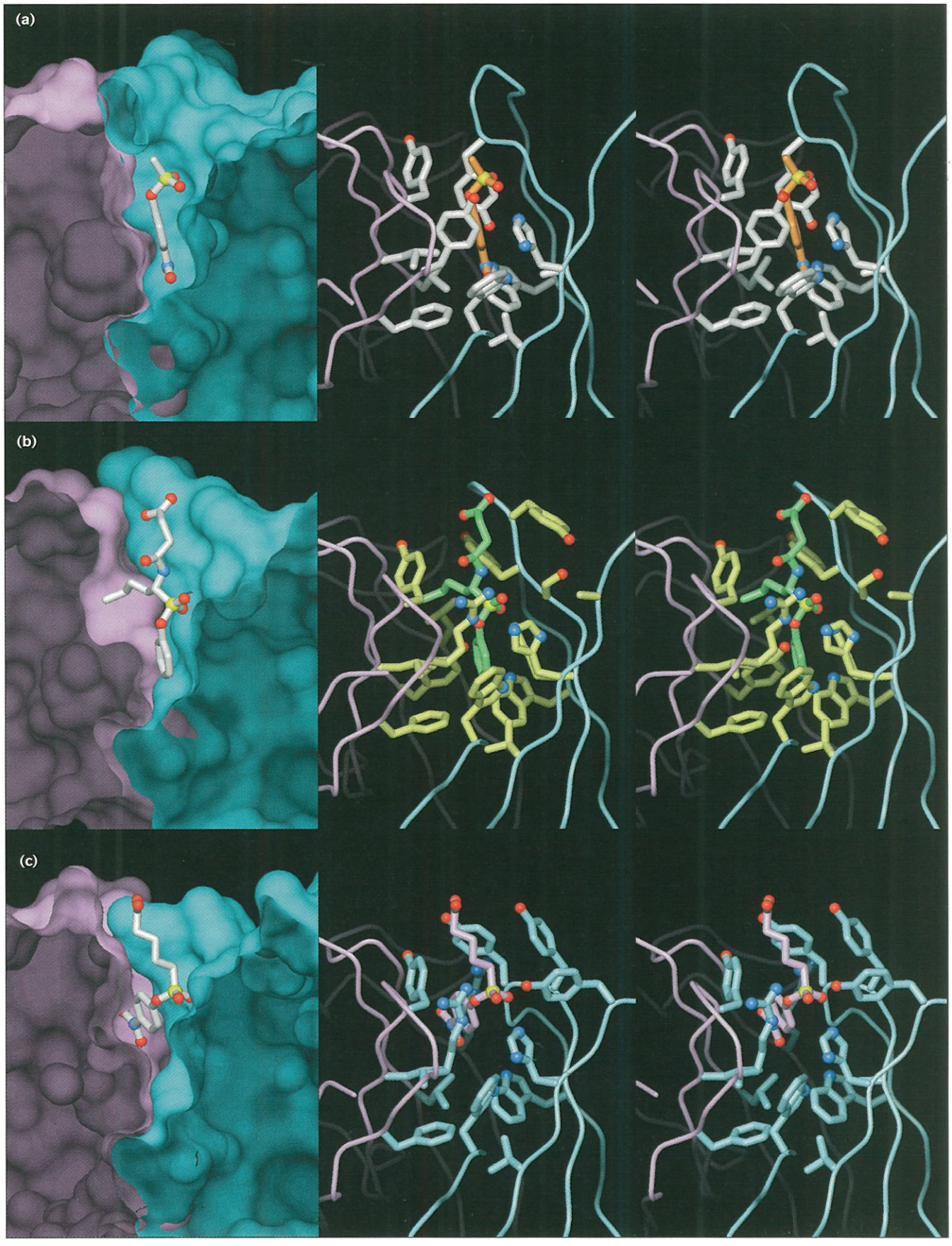
(a)
(b)
(c)

Figure 4 (facing page)

Crystal structures of three hydrolytic antibodies complexed with their cognate haptens. **(a)** CNJ206 [13], **(b)** 17E8 [19], **(c)** 48G7 [24]. The backbone and surface rendering of the heavy and light chains of each antibody are shown in cyan and pink, respectively. Left panel: Connolly surface representation of the antibodies, using a solvent sphere of radius 1.4 Å. Center and right panels: Stereo pair, displaying the side chains of active site residues identified in Table 2. Of the residues that bind the ligand, only residue H98 in CNJ206 and residue L49 in 17E8 and 48G7 have been omitted for clarity; these make relatively unimportant contacts with the alkyl group of the hapten.

the antibody is bell-shaped, suggesting that two ionizable groups may be involved in catalysis.

Despite the differences in their haptens, CNJ206 and 17E8 exhibit striking similarities in their combining sites (Fig. 4,5a). As with CNJ206, 17E8 binds its hapten with the aryl leaving group buried deeply at the bottom of an apolar binding pocket (Fig. 4b) [19], and uses many of the same residues as CNJ206 to form this site. In the CNJ206•**1b** complex, five residues come within 3.5 Å of the *p*-nitrophenyl moiety of the ligand: LeuL89, HisH35, ValH37, TrpH47, and TrpH103. Significantly, all five of these important binding-site residues are identical in 17E8 (Table 2). Moreover, among the 10 residues in total that contact the arylphosphonate moiety of the hapten in CNJ206, seven are identical in 17E8 and another is changed conservatively (GlyH95→Ser). This contrasts with a more modest overall sequence identity of 48 % for the heavy chain variable region (V_H) and 59 % for that of the light chain (V_L). The high degree of sequence conservation in the active site arises in part from the fact that both antibodies enlist several framework residues to form the base of the binding pocket (Table 2). Nevertheless, many CDR residues are also conserved, as is the overall mode of hapten binding. As expected, greater individuality is seen in those regions that contact components of the two haptens that are not common to both. The many similarities are remarkable, however, and raise some interesting questions.

Clearly, the response of the immune system to the two arylphosphonate haptens has a common theme, even though the germline sequences that were used to generate the two antibodies are different. Does this indicate a strong bias in the immune system, predisposing the response to a particular solution or family of solutions? The fact that several framework residues are used in the active site supports this hypothesis. It has been estimated that the primary immunoglobulin repertoire contains ~10^8 different antibodies and that this diversity is further expanded by several orders of magnitude through the process of somatic hypermutation [20,21]. However, the presence of a preformed pocket able to accommodate the aryl group in haptens such as these may quickly restrict the primary response to a much narrower subset of structures. Within this subset or 'theme', the variation of a few key residues could then lead to the observed differences in binding and catalytic properties.

For catalysis, the important variations should be in residues that form stabilizing contacts with the phosphonyl oxygens of the transition-state analog. Comparing 17E8 with CNJ206, it is clear that 17E8 provides more extensive interactions with the phosphonate group than does CNJ206 (Fig. 6). In addition to the hydrogen bond from the backbone NH of H96 (which is present in both antibodies), the side chains of two cationic residues, LysH93 and ArgL96, provide complementary electrostatic/hydrogen bonding interactions with the pro-S and pro-R phosphonyl oxygens, respectively. It is likely that these interactions account for the greater catalytic efficiency afforded by 17E8 relative to CNJ206 (Table 1). Cationic residues are known to be very effective in stabilizing oxyanions. In the case of carboxypeptidase A, mutagenesis of a single arginine residue implicated in oxyanion binding resulted in a 20 000-fold loss of activity [22,23]. In addition, the side chain of ArgL96 appears poised to complement the incipient negative charge on the phenolate oxygen. In CNJ206, this residue is replaced by a tyrosine, which is less able to accommodate the negative charge. Electrostatic stabilization of the leaving group may thus explain the ability of 17E8, but not CNJ206, to

Table 1

Kinetic parameters for the four hydrolytic antibodies discussed in the text.

Antibody	Substrate	pH	k_{cat}/K_M (M^{-1} min^{-1})	k_{cat} (min^{-1})	k_{cat}/k_{uncat}	Reference
CNJ206	**2b**	8.0	5000	0.4	1600	12
48G7	**10a**	8.2	14 000	5.5	16 000	24
17E8	**6**, X = CH_2	8.7	390 000	100	13 000	18
43C9	**14**, X = O	9.3	28 000 000	1500	27 000	29,32
43C9	**14**, X = NH	9.0	140	0.08	250 000	28,32

Figure 5

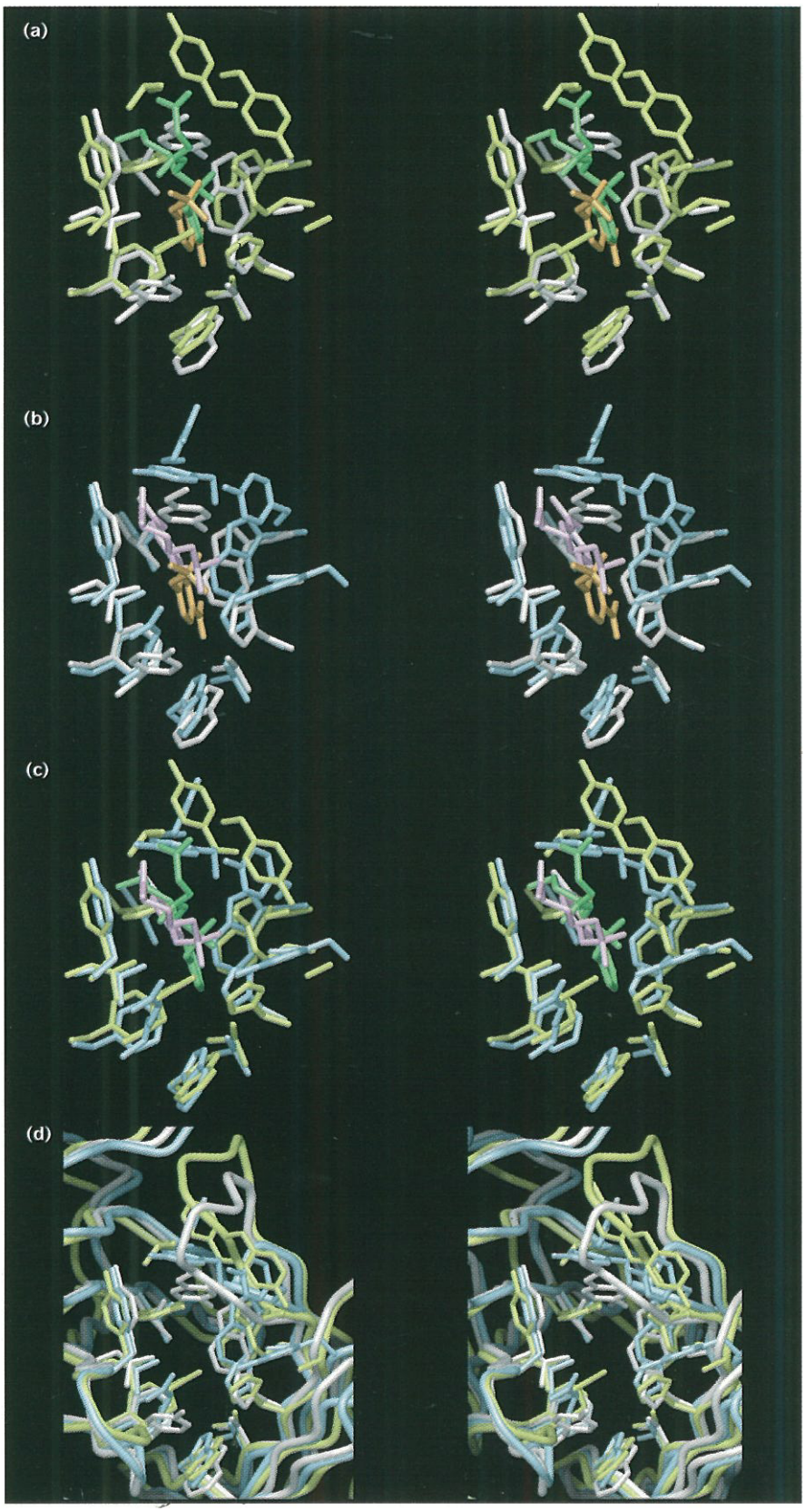

The binding sites of the three st
characterized hydrolytic antibod
remarkably similar. **(a)–(c)** Pair-
of the hydrolytic antibodies com
their respective haptens. CNJ2(
white, with hapten **1b** in orange
shown in yellow, with hapten **5** i
48G7 is shown in cyan, with ha
pink [24]. **(d)** Overlay of all thre
17E8 and 48G7 were superim
CNJ206 using all the heavy ato
conserved active site residues L
TyrL91, PheL98, HisH35, ValH
and Trp H103 (root-mean-squa
152 atoms of 1.01 Å for 17E8/(
1.05 Å for 48G7/CNJ206).

Table 2

Sequence comparison of the active site residues of four hydrolytic antibodies.

Residue	Location[a]	CNJ206	48G7	17E8	43C9
L36	FR2	L	L	Y	**Y**
L89	CDR3	L	L	L	**Q**
L96	CDR3	Y	R	R	**R**
L98	FR4	**F**	**F**	F	**F**
H33	CDR1	**G**	Y	**A**	**N**
H35	CDR1	H	H	H	**H**
H37	FR2	V	**V**	V	**V**
H47	FR2	W	**W**	W	**W**
H93	FR3	**A**	**A**	K	**V**
H95	CDR3	G	Y	S	**Y**
H103	FR4	W	**W**	W	**W**
L34	CDR1	**S**	G	G	**A**
L46	FR2	**R**	R	L	**L**
L49	FR2	**Y**	Y	H	**Y**
L91	CDR3	Y	Y	Y	**H**
H96	CDR3	D	Y	Y	**G**
H97	CDR3	Y	Δ	Y	**Y**
H98	CDR3	Y	G	G	**G**

Residues are colored to indicate the parts of the haptens to which they make the most contacts: arylphosphonate moiety blue, linker pink, and alkyl side chain green. TyrH96 makes significant contacts with both the arylphosphonate and linker moieties in 48G7 and is colored accordingly. Contact residues were identified by the program CONTACSYM [58], using a distance threshold of 4.33 Å.
[a]FR, framework region; CDR, complementarity determining region.

catalyze the hydrolysis of unsubstituted aryl esters. The simplest interpretation of these observations is that 17E8 functions in a manner similar to that predicted for CNJ206, with direct hydroxide attack on the scissile carbonyl promoted by numerous stabilizing interactions with the resulting oxyanion. The more extensive interactions afforded by 17E8 would then account for its increased efficacy.

An alternative mechanism for 17E8 has been proposed, involving rate-limiting formation of a covalent acyl-antibody intermediate [18,19]. Modeling studies based on the structure of the antibody–hapten complex led to the hypothesis that SerH95 is transiently acylated during catalysis [19]. Since it is observed to be hydrogen-bonded to TyrH97 and directed out of the binding pocket in the crystal structure, the proposed mechanism involves a novel pH switch. The tyrosine becomes deprotonated at high pH, freeing the serine to rotate into the active site. It was suggested that HisH35 could then act as a general base and activate the serine for nucleophilic attack on the substrate's scissile carbonyl.

Although an appealing analogy can be made between this Ser-His dyad and the Ser-His-Asp catalytic triad of serine proteases [19], the hypothesis must be viewed with some skepticism for a number of reasons. First, the mechanism is based on hydroxylamine partitioning data, which show inconsistencies between the hydroxylamine-dependent rates of phenol release and quantitation of the hydroxamic acid product [18]. Second, there is no apparent chemical advantage to forming an alkyl ester as an intermediate in the cleavage of the relatively labile aryl-ester substrate 6. It is also unclear why hydrolysis of such an intermediate would be faster than its formation. Third, if HisH35 is to participate in the proposed mechanism, it must break a highly conserved hydrogen bond with the indole NH of framework residue TrpH47. This interaction is preserved in many antibody structures, including

Figure 6

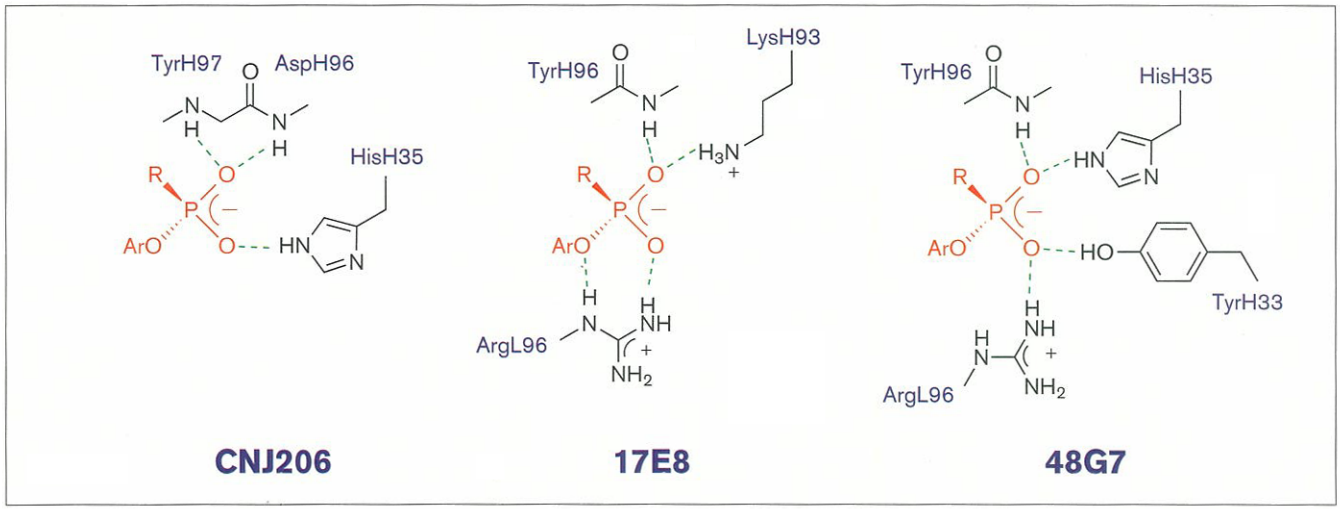

Schematic depiction of the hydrogen bonds and salt bridges formed with the phosphonate moiety of the bound haptens in three hydrolytic antibodies. The interactions are inferred from the crystal structures of the complexed antibodies and are expected to be important for transition-state stabilization during ester hydrolysis.

those of CNJ206 [13] and 48G7 [24] (discussed below). Finally, a closely related antibody, 29G11, which has a glycine at position H95 but is otherwise identical to 17E8 in all other active site residues [25], is only four-fold less active than 17E8 and exhibits a similar pH–rate profile. The suggestion that 17E8 forms a covalent acyl intermediate consequently seems unlikely, unless more evidence can be provided in its favor.

48G7: variation in the mode of binding

The similarity between CNJ206 and 17E8 leads us to ask how much variation we can expect to see among other antibodies obtained using similar haptens. For example, will all such antibodies employ the same conserved pocket to bind the aryl leaving group, or can this vary to some extent? The recent structure of a third esterolytic antibody provides us with further insights.

Antibody 48G7 [26] was generated against the *p*-nitrophenyl phosphonate hapten **9a**, nearly identical to the hapten used to produce CNJ206. It accelerates the hydrolysis of activated ester **10a** and carbonate **10b** by factors of 1.6×10^4 and 4×10^4 respectively, falling between CNJ206 and 17E8 with respect to its catalytic properties (Table 1). Sequence comparison between 48G7 [26] and the other two antibodies [12,18] reveals a high degree of conservation in the binding-site residues. Of the ten amino acids in CNJ206 that contact the arylphosphonate moiety of the bound hapten, seven are identical in 48G7. The same is seen for 17E8, where eight of the ten contact residues are preserved in 48G7 (Table 2). Again, the overall sequence identity among the three antibodies is more modest, although CNJ206 and 48G7 appear to share a common light chain (92.5% sequence identity for V_L).

Given the degree of sequence conservation among active-site residues, we might expect 48G7 to bind its ligand in the same way as do CNJ206 and 17E8. Surprisingly, this is not the case. Although the cavity that accommodates the aryl moiety of the hapten in both CNJ206 and 17E8 is also found in 48G7, it lies empty (Fig. 4c) [24]. The phosphonyl group occupies the same location, but the aryl group is turned, lying in an adjacent pocket not present in CNJ206. We cannot, however, rule out the possibility that the productive mode of substrate binding is different, since the crystal structure provides only a static picture of a dynamic system. It is interesting that the second pocket is also present in 17E8, where it accommodates the alkyl side chain of hapten **5** (Fig. 4b). 48G7 might therefore catalyze the hydrolysis of phenyl or *p*-nitrophenyl esters of L-norleucine, L-methionine, or L-phenylalanine. The presence of a branched side chain in the substrate would force the leaving group to bind in the unoccupied cavity of 48G7, mimicking the binding mode of 17E8.

Despite the variation in ligand orientation observed in 48G7, the overall theme is maintained: the apolar binding pocket is conserved (though unoccupied), the aryl moiety of the hapten is buried, and the phosphonate group is held in place through specific electrostatic and hydrogen bonding interactions near the mouth of the pocket. In fact, when the three antibody structures are overlaid, the phosphonate groups of the bound haptens occupy a similar location (Fig. 5). Not surprisingly, the largest differences are seen in the heavy-chain CDR3 loop, but these differences do not affect the overall motif. With respect to catalysis, important variations are evident in how the antibodies bind the phosphonate group and hence are expected to stabilize the corresponding transition-state species (Fig. 6). Like CNJ206 and 17E8, 48G7 uses the backbone NH of residue H96 to bind the pro-S oxygen of the hapten. In addition, the imidazole group of HisH35 donates a second hydrogen bond to this oxygen. The pro-R oxygen is stabilized by a salt bridge with ArgL96 (seen in 17E8) and a hydrogen bond with the side chain of TyrH33. The latter interaction is unique to 48G7; CNJ206 and 17E8 have a glycine and an alanine in this position, respectively.

As for CNJ206 and 17E8, the most likely mechanism for 48G7 involves direct hydroxide attack on the scissile carbonyl of the substrate. Mutagenesis studies on 48G7 have investigated the importance of HisH35, ArgL96, and TyrH33 for catalysis: changing these residues respectively to Glu, Gln, and Phe results in a reduction in k_{cat} of 30-, 11-, and 3.2-fold [24]. The effects for ArgL96 and TyrH33 are relatively small, and it has been proposed that this reflects the ability of one residue to compensate for the other when one of the interactions with the oxyanion is lost [24]. However, high solvent accessibility and/or conformational mobility of these residues could also account for the results.

43C9: covalent catalysis, an unexpected variation

The simple mechanism employed by CNJ206, 17E8, and 48G7 arises directly from the common strategy used to generate the catalysts. The phosphonate hapten programs for direct hydroxide attack on the corresponding substrate, facilitated by specific stabilizing interactions with the oxyanionic transition-state species. It is surprising, then, that we observe a more sophisticated mechanism employed by a fourth hydrolytic antibody, 43C9 [27].

Analogous to the other three catalysts, 43C9 was generated using phosphonamidate hapten **13**, designed to mimic the transition-state species formed during the hydrolysis of *p*-nitroanilides (Fig. 2) [28]. This catalyst is one of the most active hydrolytic antibodies reported to date and a rare example of an amidase. At pH 9.0, 43C9 accelerates the hydrolysis of *p*-nitroanilide **14** by a factor of 2.5×10^5 (k_{cat}/k_{uncat}) [28]. It also hydrolyzes the

corresponding ester substrate, albeit with somewhat diminished efficiency relative to the uncatalyzed reaction ($k_{cat}/k_{uncat} = 2.7 \times 10^4$) [29]. Mutagenesis experiments [30,31] and extensive steady-state and pre-steady-state kinetic data [27,32] support a two-step mechanism. In the first step, nucleophilic attack of the substrate by an active-site histidine yields a covalent acyl-antibody intermediate. Deacylation by hydroxide ion in the second step releases the acid product and regenerates the antibody catalyst. The intermediate does not accumulate under most conditions, but was detected by electrospray mass spectrometry at pH 5.9 [33].

Although no crystal structure of 43C9 complexed with its hapten is available, homology modeling has been applied in an effort to understand this catalyst's unique properties [30]. The model of 43C9 was constructed in a step-wise fashion using an antibody structural database. First, appropriate framework residues were selected based on sequence comparison. Then, the CDRs were modeled using structural templates from antibodies with closely related sequences. Although the conformation of five of the CDRs could be predicted with reasonable confidence, CDRH3 could not be modeled successfully since highly homologous sequences were unavailable. Nevertheless, the V_H and V_L domains were paired and the hapten docked into the active site. In a final step, the H3 loop was optimized by manual adjustment and energy minimization of the side-chain positions.

Sequence comparison of 43C9 [34] with each of the other hydrolytic antibodies discussed above reveals a reasonably high degree of conservation among active-site residues (Table 2). In particular, 43C9 most closely resembles 17E8. Of the 10 residues that contact the aryl moiety of the hapten in 17E8, 7 are identical in 43C9 and another is altered conservatively (LeuL89→Gln). As we might expect, the homology model of 43C9 has many similarities to the crystal structure of 17E8. Where the model deviates most is in the conformation of CDRH3 and in the orientation of the bound hapten (Fig. 7). Notably, this is also where the greatest uncertainty in the model lies, due to the unavailability of suitable structural templates for the CDRH3 loop and to the possibility of substantial ligand-induced conformational changes in the binding site (as exemplified by CNJ206, Fig. 3). In the model of 43C9, the hydrophobic pocket that is used to bind the aryl leaving group in 17E8 (and CNJ206) is occupied by the side chains of two CDRH3 residues, PheH100b and TyrH95. Hapten **13** was therefore docked in a rather shallow depression on the antibody surface to allow the formation of a salt bridge between its phosphonate moiety and the guanidinium group of ArgL96 [30]. Although a distinctive binding mode for this ligand cannot be ruled out, it seems equally plausible that the modeled conformation of the H3 loop is incorrect and that 43C9 recognizes its hapten in much the same way as 17E8, burying the aryl leaving group deep within the combining site and forming numerous stabilizing interactions with the phosphonamidate moiety near the mouth of the active site. This hypothesis would help to explain the finding that *p*-nitrophenol release limits the rate of ester hydrolysis at high pH.

The unprogrammed mechanism of 43C9 leads us to ask what distinguishes it from the other three hydrolytic antibodies. Extensive mutagenesis studies on 43C9 have revealed the importance of three active-site residues. Changing ArgL96 to Gln resulted in a >20-fold loss in

Figure 7

Stereo pair showing the crystal structure of 17E8 [19], superimposed on the homology model of 43C9 [30]. 17E8 is shown in yellow, with hapten **5** in green. 43C9 is shown in pink, with hapten **13** in blue. The overlay demonstrates the similarities between the two antibodies, as well as the difference in the predicted binding mode of hapten **13** in 43C9 relative to that of hapten **5** in 17E8. The structures were superimposed using the backbone atoms of residues L89, L91, L98, H35, H37, H47, and H103 (root-mean-square deviation of 0.56 Å for 56 atoms).

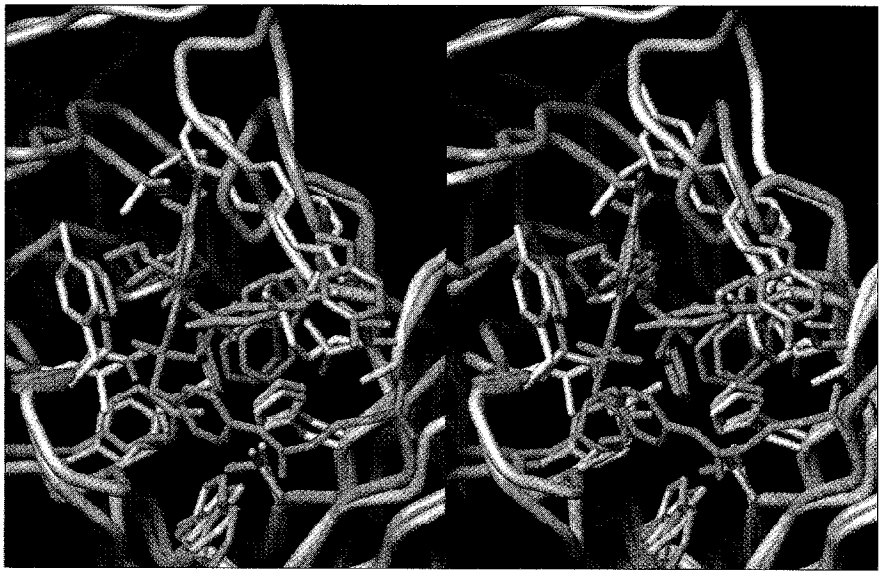

activity, consistent with its importance in transition-state stabilization [30]. This arginine is also present in 17E8 and 48G7, where it presumably has a similar role. Mutagenesis of two histidine residues, HisH35 and HisL91, also yielded inactive variants of 43C9 [31]. Interestingly, substitutions for HisH35 not only affected catalysis but also gave proteins with substantially reduced affinities for the hapten and products. In contrast, modifications of HisL91 had little effect on binding. These results were interpreted in favor of a structural role for HisH35 and a catalytic role for HisL91 as the active-site nucleophile. Failure to detect a covalent intermediate by electrospray mass spectrometry when a HisL91→Gln mutant was incubated with the ester substrate has been cited as further evidence for the transient acylation of HisL91 during catalysis [32].

Nucleophilic catalysis may explain why 43C9, but not 17E8, can cleave an acyl derivative that contains the relatively poor *p*-nitroanilide leaving group. Although this is not programmed by the hapten, 43C9 adopts a similar strategy to that used by serine proteases, dividing a difficult reaction into a series of more tractable steps. Since 17E8 is so similar in its combining site to 43C9, it would be interesting to replace TyrL91 in 17E8 with a histidine residue to determine whether the properties of the mutated antibody approximate those of 43C9. In a complementary experiment, introduction of a lysine residue in place of ValH93 in 43C9 might provide additional transition-state stabilization.

Evolution of the immune response

The structural and biochemical information for the hydrolytic antibodies discussed above has contributed significantly to our understanding of antibody-mediated hydrolysis of esters and amides. In particular, we have learned that the immune system adopts a common theme in constructing an appropriate binding site for these related ligands. Within this motif, variations are observed that must account for the differences in catalytic efficiency. Each antibody employs its own set of interactions for transition-state stabilization, some of which are shared by the other catalysts and some of which are unique (Fig. 6). In this respect, the antibodies resemble the products of convergent evolution.

The emergence of a principal theme among different antibodies that recognize the same ligand has also been observed in a number of model studies. When A/J strain mice are immunized with a protein conjugate of *p*-azophenylarsonate, most of the antibodies produced share a cross-reactive idiotype that results from the combination of a single set of gene segments: V_H Id^{CR}, $DFL_{16,1e}$ and J_H2 for the heavy chain, and V_K10 and J_K1 for the light chain [35]. The murine immune response to 2-phenyl oxazolone (phOx) is also dominated by a particular combination of heavy and light chain V regions (dubbed V_H-Ox1 and V_K-Ox1) [36]. Interestingly, when a phOx-binding antibody was found with a unique V_H region (only 48 % homologous to V_H-Ox1), its structure showed that important antigen-binding residues had been conserved [37]. This parallels the similarities noted among the four hydrolytic antibodies discussed here, where sequence conservation is generally greatest among ligand-contacting residues. Extensive sequence analysis of other phOx-binding antibodies led to the conclusion that the mouse immune system uses a very limited number of principal mechanisms to recognize this antigen [37]. A similar conclusion was reached by Padlan *et al.* [38] based on analogous studies with mouse anti-phosphorylcholine antibodies. Apparently, the strong selective pressure imposed by the immune system quickly reduces the broad diversity initially present in the antibody repertoire to a small number of the best solutions.

Is binding-site diversity increased significantly as the immune response is refined through somatic hypermutation? To answer this, we must compare mature, high-affinity antibodies with their germline precursors. This was recently accomplished for 48G7; the parent antibody was cloned, sequenced, and expressed [24]. It was found that, during the course of affinity maturation, nine amino acid changes had accumulated in its variable domain, six in the heavy chain and three in the light chain. The germline antibody bound its hapten with a dissociation constant (K_d) of 135 μM; the mature antibody, 48G7, had a K_d of 4.5 nM. As expected, the catalytic efficiency of the antibody improved as its affinity for the transition-state analog increased. However, the 30 000-fold increase in affinity from germline to mature antibody only gave an 82-fold increase in the apparent second-order rate constant, k_{cat}/K_M. Thus, only a small fraction of the newly acquired binding affinity is used for transition-state stabilization.

How did the process of somatic hypermutation lead to the increase in affinity? In the crystal structure of the 48G7•**9a** complex, none of the nine residues that were altered during affinity maturation makes direct contact with the ligand. Although six of the nine mutations occur in the CDRs, the residues surround the binding pocket. Similar results have been obtained in other studies of somatic mutations [35–37,39]. In each case, most or all of the changes occur in residues that are not in direct contact with the hapten. Recently, Winter and coworkers [40] carried out an extensive analysis of the entire human V_H and V_K repertoires. They compiled a database of 1181 rearranged V_H and 736 rearranged V_K sequences and identified the location of somatic mutations in each sequence. Mapping this information onto the structure of a representative antibody led to the conclusion that

sequence diversity is focused at the center of the binding site in the primary repertoire, but spreads to regions at the periphery of the binding site during somatic hypermutation. They propose that 'evolution has favored this complementarity as an efficient strategy for searching sequence space'. The changes that accumulate as the antibodies are refined probably either reorganize the active-site residues via conformational changes, optimizing their geometries for hapten binding, or limit the flexibility of the active-site loops, reducing the entropic cost incurred by binding the ligand.

Implications

In the case of 48G7, all the important residues involved in transition-state stabilization were already present in its germline precursor. The process of affinity maturation served mainly to refine the existing motif, presumably by 'tightening' the structure through improved packing and secondary hydrogen-bonding interactions. Does this suggest that the immune system is intrinsically limited as a source of highly active catalysts? Enzymes like subtilisin, a natural counterpart of hydrolytic antibodies, use complex constellations of residues that are precisely aligned for catalysis in their active sites [41,42]. Such arrays may be unavailable in the primary repertoire of the immune system and (given the results discussed here) may not be accessible through somatic hypermutation.

At present, it is not clear how much activity can be obtained from the motif shared by the antiphosphonate antibodies. We have seen that different residues may be used to stabilize the transition state, with differing degrees of effectiveness. Moreover, the study of 43C9 shows that unprogrammed mechanisms analogous to those used by natural enzymes can arise, albeit through serendipity. Yet, although 43C9 is quite a sophisticated catalyst, it is still primitive compared to highly-evolved enzymes like subtilisin. For example, *p*-nitroanilide hydrolysis by 43C9 (k_{cat} = 1.3×10^{-3} s^{-1} at pH 9.0, 37 °C [28]) is more than 30 000 times less efficient than the subtilisin-catalyzed cleavage of succinyl-Ala-Ala-Pro-Phe-*p*-nitroanilide (k_{cat} = 44 s^{-1} at pH 8.0, 25 °C [16]). Can we expect to bridge this gap, or are we forever limited by the bounds imposed by the immune system?

If we are to achieve the goal of enzyme-like efficiency, it may be necessary to explore new approaches for optimizing catalytic activity. In the case of ester and amide hydrolysis, we have learned that a common theme presents itself in response to the haptens employed in these studies. The phosphonate moiety is positioned near the mouth of the pocket, with the phosphonyl oxygens directed laterally and the leaving group deeply buried. In contrast to this, several natural proteases, including carboxypeptidase A [43], thermolysin [44], and α-lytic protease [45], bind phosphonate inhibitors with the phosphonyl oxygens directed toward the base of the pocket and the leaving group and acid moieties positioned laterally. To mimic this mode of binding, we may have to use novel haptens that provide access to different subsets of the primary immunoglobulin repertoire. Alternatively, *in vitro* selection methods, such as phage display technology [46], can free us from the particular predispositions of the immune system (although they may introduce new biases). Semisynthetic antibody libraries [47,48], or even libraries composed of receptors completely unrelated to the immunoglobulin fold, may also be used to obtain novel binding sites [49].

New functional groups could conceivably be introduced into first-generation antibody catalysts by site-directed mutagenesis. This offers a way to circumvent the low probability of obtaining complex constellations of catalytic residues in a single step. Heterologous immunization [50] and the use of mechanism-based inhibitors as templates [51] may also allow the induction of multiple properly oriented catalytic residues. The use of organic cofactors [52,53] or metal ions [54] presents an alternative way to promote energetically demanding chemical transformations. In concert with such approaches, it may be necessary to alter the strategy of selection. Comparing $\log(k_{cat}/k_{uncat})$ with $\log(K_M/K_i)$ for a wide range of antibody catalysts indicates that as the affinity of the antibody for its hapten increases (K_i gets smaller), a lower proportion of the binding energy is used to stabilize the transition state relative to the ground state of the substrate [55]. This emphasizes the need to optimize existing catalysts by selecting directly for catalytic activity [26,56,57] instead of for affinity for an inevitably imperfect transition-state analog. An incremental approach will probably be required in which modest catalysts are improved by multiple rounds of mutagenesis and selection.

Attempts to produce more efficient catalytic antibodies through alternative strategies such as these will benefit greatly from the accumulating biochemical and structural data. For the antibodies discussed above, such information has already ratified the basic approach taken to generate these catalysts and provides us with the mechanistic understanding we need to direct our future efforts. Continued probing of these active sites, coupling mutagenesis with structure determination, promises to provide additional insight, not only into antibody-mediated hydrolysis, but into the promotion of hydrolytic reactions more generally.

Acknowledgements

Support of this work by the National Institutes of Health is gratefully acknowledged. G.M. is the recipient of a Natural Sciences and Engineering Research Council of Canada 1967 Centennial Postgraduate Scholarship. We also thank Mike Pique for his enthusiastic and invaluable help with the graphics.

References

1. Perlmann, G.E. & Lorand, L., eds (1970). Proteolytic enzymes. In *Methods in Enzymology*. (Colowick, S.P. & Kaplan, N.O., eds), Academic Press, Inc., New York.
2. Lorand, L., ed. (1976). Proteolytic enzymes: Part B. In *Methods in Enzymology*. (Colowick, S.P. & Kaplan, N.O., eds), Academic Press, Inc., New York.
3. Lorand, L., ed. (1981). Proteolytic enzymes: Part C. In *Methods in Enzymology*. (Colowick, S.P. & Kaplan, N.O., eds), Academic Press, Inc., New York.
4. Jencks, W.P. (1969). *Catalysis in Chemistry and Enzymology*. McGraw Hill, New York.
5. Lerner, R.A., Benkovic, S.J. & Schultz, P.G. (1991). At the crossroads of chemistry and immunology: catalytic antibodies. *Science* **252**, 659–667.
6. Schultz, P.G. & Lerner, R.A. (1995). From molecular diversity to catalysis: lessons from the immune system. *Science* **269**, 1835–1842.
7. Jacobsen, N.E. & Bartlett, P.A. (1981). A phosphonamidate dipeptide analogue as an inhibitor of carboxypeptidase A. *J. Am. Chem. Soc.* **103**, 654–657.
8. Kaplan, A.P. & Bartlett, P.A. (1991). Synthesis and evaluation of an inhibitor of carboxypeptidase A with a K_i value in the femtomolar range. *Biochemistry* **30**, 8165–8170.
9. Bartlett, P.A. & Marlowe, C.K. (1983). Phosphonamidates as transition-state analogue inhibitors of thermolysin. *Biochemistry* **22**, 4618–4624.
10. Sampson, N.S. & Bartlett, P.A. (1991). Peptidic phosphonylating agents as irreversible inhibitors of serine proteases and models of the tetrahedral intermediates. *Biochemistry* **30**, 2255–2263.
11. Goding, J.W. (1983). *Monoclonal Antibodies: Principles and Practice*. Academic Press, Inc., New York.
12. Zemel, R., Schindler, D.G., Tawfik, D.S., Eshhar, Z. & Green, B.S. (1994). Differences in the biochemical properties of esterolytic antibodies correlate with structural diversity. *Mol. Immunol.* **31**, 127–137.
13. Charbonnier, J.-B., *et al.*, & Knossow, M. (1995). Crystal structure of the complex of a catalytic antibody Fab fragment with a transition-state analog: structural similarities in esterase-like catalytic antibodies. *Proc. Natl. Acad. Sci. USA* **92**, 11721–11725.
14. Golinelli-Pimpaneau, B., *et al.*, & Knossow, M. (1994). Crystal structure of a catalytic antibody Fab with esterase-like activity. *Structure* **2**, 175–183.
15. Kabat, E.A., Wu, T.T., Reid-Miller, M., Perry, H.M. & Gottesman, K.S. (1987). *Sequences of proteins of immunological interest*. National Institutes of Health, Bethesda, MD.
16. Bryan, P., Pantoliano, M.W., Quill, S.G., Hsiao, H.-Y. & Poulos, T. (1986). Site-directed mutagenesis and the role of the oxyanion hole in subtilisin. *Proc. Natl. Acad. Sci. USA* **83**, 3743–3745.
17. Wells, J.A., Cunningham, B.C., Graycar, T.P. & Estell, D.A. (1986). Importance of hydrogen-bond formation in stabilizing the transition state of subtilisin. *Philos. Trans. R. Soc. Lond. (A)* **317**, 415–423.
18. Guo, J., Huang, W. & Scanlan, T.S. (1994). Kinetic and mechanistic characterization of an efficient hydrolytic antibody: evidence for the formation of an acyl intermediate. *J. Am. Chem. Soc.* **116**, 6062–6069.
19. Zhou, G.W., Guo, J., Huang, W., Fletterick, R.J. & Scanlan, T.S. (1994). Crystal structure of a catalytic antibody with a serine protease active site. *Science* **265**, 1059–1064.
20. Alt, F.W., Blackwell, T.K. & Yancopoulos, G.D. (1987). Development of the primary antibody repertoire. *Science* **238**, 1079–1087.
21. Rajewsky, K., Förster, I. & Cumano, A. (1987). Evolutionary and somatic selection of the antibody repertoire in the mouse. *Science* **238**, 1088–1094.
22. Phillips, M.A., Fletterick, R. & Rutter, W.J. (1990). Arginine 127 stabilizes the transition state in carboxypeptidase A. *J. Biol. Chem.* **265**, 20692–20698.
23. Phillips, M.A., Kaplan, A.P., Rutter, W.J. & Bartlett, P.A. (1992). Transition-state characterization: a new approach combining inhibitor analogues and variation in enzyme structure. *Biochemistry* **31**, 959–963.
24. Patten, P.A., *et al.*, & Schultz, P.G. (1996). The immunological evolution of catalysis. *Science* **271**, 1086–1091.
25. Guo, J., Huang, W., Zhou, G.W., Fletterick, R.J. & Scanlan, T.S. (1995). Mechanistically different catalytic antibodies obtained from immunization with a single transition-state analog. *Proc. Natl. Acad. Sci. USA* **92**, 1694–1698.
26. Lesley, S.A., Patten, P.A. & Schultz, P.G. (1993). A genetic approach to the generation of antibodies with enhanced catalytic activities. *Proc. Natl. Acad. Sci. USA* **90**, 1160–1165.
27. Benkovic, S.J., Adams, J.A. & Borders, C.L., Jr. (1990). The enzymic nature of antibody catalysis: development of multistep kinetic processing. *Science* **250**, 1135–1139.
28. Janda, K.D., Schloeder, D., Benkovic, S.J. & Lerner, R.A. (1988). Induction of an antibody that catalyzes the hydrolysis of an amide bond. *Science* **241**, 1188–1191.
29. Gibbs, R.A., Benkovic, P.A., Janda, K.D., Lerner, R.A. & Benkovic, S.J. (1992). Substituent effects on an antibody-catalyzed hydrolysis of phenyl esters: further evidence for an acyl-antibody intermediate. *J. Am. Chem. Soc.* **114**, 3528–3534.
30. Roberts, V.A., Stewart, J., Benkovic, S.J. & Getzoff, E.D. (1994). Catalytic antibody model and mutagenesis implicate arginine in transition-state stabilization. *J. Mol. Biol.* **235**, 1098–1116.
31. Stewart, J.D., Roberts, V.A., Thomas, N.R., Getzoff, E.D. & Benkovic, S.J. (1994). Site-directed mutagenesis of a catalytic antibody: an arginine and a histidine residue play key roles. *Biochemistry* **33**, 1994–2003.
32. Stewart, J.D., Krebs, J.F., Siuzdak, G., Berdis, A.J., Smithrud, D.B. & Benkovic, S.J. (1994). Dissection of an antibody-catalyzed reaction. *Proc. Natl. Acad. Sci. USA* **91**, 7404–7409.
33. Krebs, J.F., Siuzdak, G. & Dyson, H.J. (1995). Detection of a catalytic antibody species acylated at the active site by electrospray mass spectrometry. *Biochemistry* **34**, 720–723.
34. Gibbs, R.A., *et al.*, & Benkovic, S.J. (1991). Construction and characterization of a single-chain catalytic antibody. *Proc. Natl. Acad. Sci. USA* **88**, 4001–4004.
35. Strong, R.K., Petsko, G.A., Sharon, J. & Margolies, M.N. (1991). Three-dimensional structure of murine anti-*p*-azophenylarsonate Fab 36–71. 2. Structural basis of hapten binding and idiotypy. *Biochemistry* **30**, 3749–3757.
36. Griffiths, G.M., Berek, C., Kaartinen, M. & Milstein, C. (1984). Somatic mutation and the maturation of immune response to 2-phenyl oxazolone. *Nature* **312**, 271–275.
37. Alzari, P.M., *et al.*, & Milstein, C. (1990). Three-dimensional structure determination of an anti-2-phenyloxazolone antibody: the role of somatic mutation and heavy/light chain pairing in the maturation of an immune response. *EMBO J.* **9**, 3807–3814.
38. Padlan, E.A., Cohen, G.H. & Davies, D.R. (1985). On the specificity of antibody/antigen interactions: phosphocholine binding to McPC603 and the correlation of three-dimensional structure and sequence data. *Ann. Inst. Pasteur Immunol.* **136C**, 271–276.
39. Theriault, T.P., Leahy, D.J., Levitt, M. & McConnell, H.M. (1991). Structural and kinetic studies of the Fab fragment of a monoclonal anti-spin label antibody by nuclear magnetic resonance. *J. Mol. Biol.* **221**, 257–270.
40. Tomlinson, I.M., Walter, G., Jones, P.T., Dear, P.H., Sonnhammer, E.L.L. & Winter, G. (1996). The imprint of somatic hypermutation on the repertoire of human germline V genes. *J. Mol. Biol.* **256**, 813–817.
41. Carter, P. & Wells, J.A. (1988). Dissecting the catalytic triad of a serine protease. *Nature* **332**, 564–568.
42. Wells, J.A. & Estell, D.A. (1988). Subtilisin – an enzyme designed to be engineered. *Trends Biochem. Sci.* **13**, 291–297.
43. Kim, H. & Lipscomb, W.N. (1991). Comparison of the structures of three carboxypeptidase A-phosphonate complexes determined by X-ray crystallography. *Biochemistry* **30**, 8171–8180.
44. Tronrud, D.E., Holden, H.M. & Matthews, B.W. (1987). Structures of two thermolysin–inhibitor complexes that differ by a single hydrogen bond. *Science* **235**, 571–574.
45. Bone, R., Sampson, N.S., Bartlett, P.A. & Agard, D.A. (1991). Crystal structures of alpha-lytic protease complexes with irreversibly bound phosphonate esters. *Biochemistry* **30**, 2263–2272.
46. Marks, J.D., Hoogenboom, H.R., Griffiths, A.D. & Winter, G. (1992). Molecular evolution of proteins on filamentous phage. *J. Biol. Chem.* **267**, 16007–16010.
47. Barbas, C.F., III, Bain, J.D., Hoekstra, D.M. & Lerner, R.A. (1992). Semisynthetic combinatorial antibody libraries: a chemical solution to the diversity problem. *Proc. Natl. Acad. Sci. USA* **89**, 4457–4461.
48. Barbas, C.F., III, Amberg, W., Simoncsits, A., Jones, T.M. & Lerner, R.A. (1993). Selection of human anti-hapten antibodies from semisynthetic libraries. *Gene* **137**, 57–62.
49. Napolitano, E.W., *et al.*, & Tainer, J.A. (1996). Glubodies: randomized libraries of glutathione transferase enzymes. *Chemistry & Biology* **3**, 359–367.
50. Tsumuraya, T., Suga, H., Meguro, S., Tsunakawa, A. & Masamune, S.

(1995). Catalytic antibodies generated via homologous and heterologous immunization. *J. Am. Chem. Soc.* **117**, 11390–11396.
51. Wagner, J., Lerner, R.A. & Barbas, C.F., III (1995). Efficient aldolase catalytic antibodies that use the enamine mechanism of natural enzymes. *Science* **270**, 1797–1800.
52. Cochran, A.G. & Schultz, P.G. (1990). Peroxidase activity of an antibody-heme complex. *J. Am. Chem. Soc.* **112**, 9414–9415.
53. Shokat, K.M., Leumann, C.J., Sugasawara, R. & Schultz, P.G. (1988). An antibody-mediated redox reaction. *Angew. Chem. Int. Ed. Engl.* **27**, 1172–1174.
54. Iverson, B.L., *et al.*, & Lerner, R.A. (1990). Metalloantibodies. *Science* **249**, 659–662.
55. Stewart, J.D. & Benkovic, S.J. (1995). Transition-state stabilization as a measure of the efficiency of antibody catalysis. *Nature* **375**, 388–391.
56. Tang, Y., Hicks, J.B. & Hilvert, D. (1991). *In vivo* catalysis of a metabolically essential reaction by an antibody. *Proc. Natl. Acad. Sci. USA* **88**, 8784–8786.
57. Smiley, J.A. & Benkovic, S.J. (1994). Selection of catalytic antibodies for a biosynthetic reaction from a combinatorial cDNA library by complementation of an auxotrophic *Escherichia coli*: antibodies for orotate decarboxylation. *Proc. Natl. Acad. Sci. USA* **91**, 8319–8323.
58. Sheriff, S., Hendrickson, W.A. & Smith, J.L. (1987). Structure of myohemerythrin in the azidomet state at 1.7/1.3 Å resolution. *J. Mol. Biol.* **197**, 273–296.